

PROGRESS IN EXPERIMENTAL STUDY OF CURRENT FILAMENTATION INSTABILITY*

Brian Allen[#], Patric Muggli, University of Southern California, Los Angeles CA 90089 USA
 Joana Martins, Luís O. Silva, GoLP/Instituto de Plasmas e Fusão Nuclear – Laboratório Associado,
 Instituto Superior Técnico, Lisboa 1049-001 PORTUGAL
 Vitaly Yakimenko, Mikhail Fedurin, Karl Kusche, Marcus Babzien, Brookhaven National
 Laboratory, Upton NY 11973 USA
 Chengkun Huang, Los Alamos National Laboratory, Los Alamos NM 87545 USA
 Warren Mori, University of California at Los Angeles Los Angeles, CA 90095 USA

Abstract

Current Filamentation Instability, CFI, is of central importance for the propagation of relativistic electron beams in plasmas. CFI could play an important role in the generation of magnetic fields and radiation in the afterglow of gamma ray bursts and also in energy transport for the fast-igniter inertial confinement fusion concept. Simulations were conducted with the particle-in-cell code QuickPIC for e^- beam and plasma parameters at the Brookhaven National Laboratory – Accelerator Test Facility, BNL-ATF. Results show that for a 2cm plasma the instability reaches near saturation. An experimental program was proposed and accepted at the BNL-ATF and an experiment is currently underway. There are three components to the experimental program: 1) imaging of the filaments, beam density, at the exit from the plasma, 2) measurement and imaging of the transverse plasma density gradient and measurement of the magnetic field and 3) identifying the radiation spectrum of the instability. Preliminary results from phase one will be presented along with the progress and diagnostic design for the following phases of the experiment.

INTRODUCTION

Current Filamentation Instability, CFI, is a basic beam-plasma instability that is purely transverse electromagnetic and that has a purely imaginary frequency. It occurs due to non-uniformities in the transverse beam and plasma profiles, which lead to unequal opposite, beam and plasma, currents and to the generation or enhancement of transverse magnetic fields. The resulting $\mathbf{v} \times \mathbf{B}$ force (\mathbf{v} - velocity of the beam or plasma current and \mathbf{B} - magnetic field) amplifies the non-uniformity of the current and drives the instability. As a result the beam breaks up into filaments with size and spacing on the order of the plasma skin depth, c/ω_{pe} (c - speed of light in vacuum and ω_{pe} - the angular plasma electron frequency)

In the Inertial Confinement Fusion, ICF, concept the compression and ignition of the fuel pellet is accomplished in a single process. The ability to separate ICF into two processes could reduce the strict requirements for the pellet fabrication tolerances and pellet illumination symmetry requirements. The Fast-

*Work supported by NSF grant 0903822

[#]brianall@usc.edu

Igniter ICF [1, 2] concept uses a guiding metal cone manufactured into the fuel pellet. When compression of the fuel pellet reaches the critical density a short high intensity laser pulse is focused into the cone. A beam of hot electrons is generated near the critical surface and the hot electrons then propagate to the core where they ignite the fusion process. The presence of CFI for this beam of hot electrons could affect the transport and energy deposition location.

The phenomena responsible for Gamma Ray Bursts (GRB's) and their associated afterglow are largely unknown. One proposed theory for the afterglow is the Fireball theory [3]. In this theory, as matter (consisting of electrons, positrons and ions) is ejected from the GRB, relativistic collisionless shocks occur between this matter resulting in the generation of large magnetic fields and radiation. The generation of magnetic fields and radiation could possibly be explained through the occurrence of the CFI.

The regime where CFI can occur is determined by two parameters, (1) the transverse beam size (σ_r) relative to the plasma skin depth and (2) the Lorentz factor, γ_0 , of the beam. For the case where the transverse beam size is smaller than the plasma skin depth ($\sigma_r < c/\omega_{pe}$) the plasma return current flows around/outside the beam, this is a regime particularly favorable for Plasma WakeField Accelerators (PWFA) and CFI does not occur. When the transverse beam size is larger than the plasma skin depth ($\sigma_r > c/\omega_{pe}$) the return current passes through the beam, creating a situation where CFI can occur. In general, the beam is subject to instabilities with a wavenumber, k , at an arbitrary angle with respect to the beam propagation velocity, v_b . Linear analysis [4] reveals that for low γ_0 beams, the dominant instability is a two stream electrostatic instability with $k \parallel v_b$. For relativistic beams, $\gamma_0 \gg 1$, the dominant instability is the CFI. Simulations reveal that for the finite beam size case (Reference 4 is for the case of an infinite beam size) CFI dominates and the filament size and spacing are on the order of the plasma skin depth.

EXPERIMENT

An experiment is underway at the Brookhaven National Laboratory – Accelerator Test Facility, BNL-ATF. The ATF was chosen for its ability to create a regime

favorable to CFI ($\sigma_r > c/\omega_{pe}$ and $\gamma_0 \gg 1$) with its 60 MeV electron beam and also allow for the study of the instability as a function of beam density (Q – beam charge, σ_r and σ_z – bunch length) and plasma density, n_e . Parameters for the ATF over-compressed e^- beam are outlined in references [6, 7]. The plasma at the ATF is produced in a capillary discharge in the lengths of 1cm or 2cm and in the range of $10^{15} < n_e < 10^{18} \text{ cm}^{-3}$. On one hand, in the experiment the transverse size is limited by the capillary diameter ($\approx 800\mu\text{m}$). However, the beam density n_b must be maximized (i.e., decrease σ_r) to increase the growth rate of the instability: $\Gamma \sim n_b \sim \sigma_r^{-2}$ [5]. On the other hand the beam radius must be large ($> c/\omega_{pe}$) to seed the instability and observe the maximum number of filaments. A possible combination is a beam radius of $\sim 100\mu\text{m}$ and a plasma density $n_e = 2.5 \times 10^{17} \text{ cm}^{-3}$ that would yield a filament size of $\sim 10\mu\text{m}$ and multiple filaments. The experiment will be setup and conducted on the ATF beam line 1.

SIMULATIONS

Simulations done with particle-in-cell (PIC) code QuickPIC [8] for the BNL-ATF over-compressed e^- beam parameters and a uniform plasma density of $2.5 \times 10^{17} \text{ cm}^{-3}$, with the simulation parameters outlined in [7], show filamentation of the beam with the filament size and spacing on the order of the plasma skin depth, $\sim 10\mu\text{m}$. Figure 1 (left) shows the beam transverse density profile at the entrance of the plasma (faint outline of a Gaussian beam), or equivalently after 2cm of propagation in vacuum (capillary or plasma exit). Figure 1 (right) shows the beam profile after 2cm of propagation in the plasma and clearly displays filamentation of the beam as a result of CFI. Simulations confirm that the filaments size and spacing scale with the plasma density (as n_e is lowered the size $\sim c/\omega_{pe}$ increases).

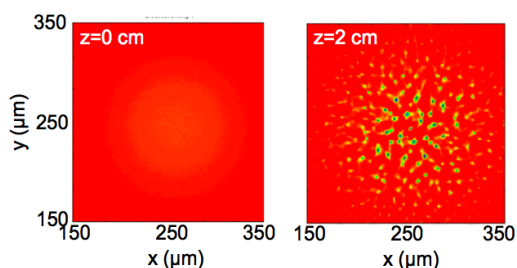


Figure 1: Transverse density for overcompressed beam parameters and a $n_e = 2.5 \times 10^{17} \text{ cm}^{-3}$: (left) Gaussian beam density at entrance to uniform plasma, (right) filamentated beam after 2 cm of propagation in plasma. Both images have the same color map.

FILAMENT IMAGING

The most direct method to observe the instability is to image the beam at its exit from the plasma (in this case exit from a capillary) and to observe filamentation of the beam. This is possible with the ATF beam due to the beams low energy density and can be realized by placing

a silicon (Si) window coated with gold (Au) at the capillary exit. The gold coating acts as a radiator generating optical transition radiation, OTR. OTR light is imaged on a CCD camera to obtain the beam/filament transverse profile. The window also allows for a sharp plasma density profile at the plasma exit. This is necessary because simulations show the filaments rapidly expand to greater than the filament spacing in the reduced plasma density expected outside of the capillary and will rejoin into a single filament. After the plasma, the filaments also rapidly expand in vacuum due to their small transverse size and large emittance. A $100\mu\text{m}$ thick Si window with a 200nm layer of Au was selected and tested [7]. Calculations show that electron scattering in the window and gold does not significantly affect the measurement of the filament's size [7].

The setup of the imaging system used in the experiment, Figure 2, consists of a Macor capillary, high magnification microscope objective and a turning mirror all placed in a vacuum chamber along beam line 1. The image is directed out of the vacuum chamber through a glass window and then transported with two additional turning mirrors onto a lens focusing on an EMCCD camera, Princeton Instruments ProEM: 1024B.

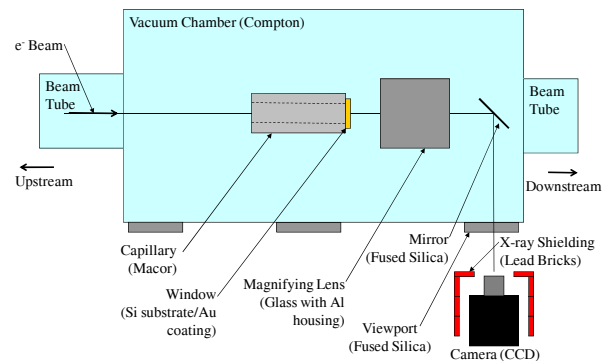


Figure 2: Longitudinal (direct) filament imaging setup at BNL/ATF on beamline 1. Inside the Compton chamber (vacuum), the system components include a Macor capillary, window made of Si, coated with Au on the downstream side, high magnification microscope objective and a turning mirror. Outside of vacuum, are turning mirrors and an EMCCD camera.

The imaging system is designed for a minimum filament diameter and spacing of $10\mu\text{m}$. For this we have a high magnification microscope objective which is vacuum compatible, Ealing 25-0506-000 with 15x magnification. The EMCCD camera has a pixel size of $13 \times 13 \mu\text{m}$.

With the full experimental setup, except for the capillary, we measured the magnification and the resolution. In place of the Si/Au window and capillary a USAF 1951 resolution test target was imaged, Figure 3. Analysis of this image reveals a magnification of 5.6x. This is the expected value for a simple two lens magnification system with the magnification defined as $M = f_1/f_2$ with f_1 and f_2 being the focal lengths of the two

lenses. The two lenses in this system are $f_{\text{lens}}=75\text{mm}$ and $f_{\text{microscope}}=13.35\text{mm}$, yielding $M=5.6\times$. For the EMCCD camera, this magnification would lead to images on the capillary window of $2.3\mu\text{m}/\text{pixel}$ and would allow for the detection of ~ 4 pixels/filament at the best resolution of the system.

We will use the definition of resolution to be the spatial frequency (line pairs/mm) where the Modulation Transfer Function, MTF, is 50% of its peak. The resolution was measured to be group 6 element 3, which corresponds to a resolution of $12.4\mu\text{m}/\text{line pair}$ or $6.2\mu\text{m}/\text{line}$. We do note that we may be pixel limited with this combination of lenses, 5 pixels/line pair and 2 or 3 pixels/line, and a longer focal length lens might be necessary for imaging small filaments ($< 10\mu\text{m}$). This has been confirmed as features of the beam/plasma interaction which are $< 10\mu\text{m}$ are not well resolved. It is important to note that going to a longer focal length lens would impact the light collection and will need to be considered.

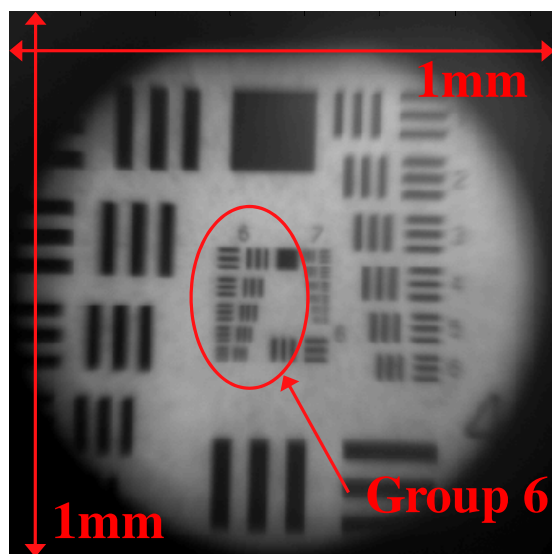


Figure 3: Longitudinal (direct) filament imaging for the imaging system setup on beamline 1, but with a USAF 1951 resolution test target placed at the location of the Si/Au window on the downstream side of the capillary.

NEXT STEPS IN THE EXPERIMENT

After direct imaging of the filaments, the next steps in the experiment are to design diagnostics and study: 1) the plasma density gradient along the length of the filaments and measure the enhanced magnetic field and 2) the radiation generated from the instability. The plasma density gradient results from the high density filaments expelling the plasma electrons and the high current filaments will result in enhancement of the magnetic field. To access these an optically transparent capillary is required, currently the capillary is made of Macor and is not transparent. When the instability is present, the particles will travel in the enhanced magnetic fields and this will lead to synchrotron radiation. Numerical

Beam Dynamics and EM Fields

Dynamics 04: Instabilities

simulations will guide the design of the radiation diagnostic diagnostic.

CONCLUSION

For the imaging system currently employed we have analyzed the magnification and resolution and found them to be sufficient for feature sizes down to $\sim 10\mu\text{m}$, which corresponds to plasma densities between 10^{14} and 10^{17}cm^{-3} . For features $< 10\mu\text{m}$ a longer focal length lens will be necessary.

Preliminary experiments with the beam and the plasma showed the appearance of beam filaments at the plasma exit with transverse size decreasing with increasing plasma density. These encouraging initial results will be reported elsewhere.

ACKNOWLEDGEMENTS

This work was supported by NSF grant 0903822 and DoE grant DEFG03-92ER40745. Simulations were conducted on HPCC at the University of Southern California and on NERSC. The authors would also like to thank the UCLA/IST collaboration team for access to QuickPIC and their support.

REFERENCES

- [1] Y. Sentoku et al., Physical Review Letters 90, 155001 (2003).
- [2] C. Deutsch et al., Transport Theory and Statistical Physics, Volume 34, Issue 3 - 5, 353 (2005).
- [3] G. Cavallo and M.J. Rees, "A qualitative study of cosmic fireballs and gamma-ray bursts", Royal Astronomical Society, Monthly Notices, 183, 359 (1978).
- [4] A. Bret et al., The Astrophysical Journal, Volume 699, Number 2, (2009).
- [5] A. Bret et al., Physical Review Letters 94, 115002 (2005).
- [6] W.D. Kimura et. al, AIP Conference Proceedings Volume 877, 534 (2006).
- [7] B. Allen et al., AIP Conference Proceedings Volume 1299 (2010).
- [8] C. Huang et. al. Journal of Computational Physics, Volume 217, Issue 2 (2006).